VIBRATING RF MEMS FOR LOW POWER WIRELESS COMMUNICATIONS

Clark T.-C. Nguyen

Center for Integrated Wireless Microsystems
Department of Electrical Engineering and Computer Science
University of Michigan
Ann Arbor, Michigan 48109-2122

ctnguyen@eecs.umich.edu

ABSTRACT

Micromechanical communication circuits fabricated via IC-compatible MEMS technologies and capable of low-loss filtering, mixing, switching, and frequency generation, are described with the intent to miniaturize wireless transceivers. Possible transceiver front-end architectures are then presented that use these micromechanical circuits in large quantities to substantially reduce power consumption. Technologies that integrate MEMS and transistor circuits into single-chip systems are then reviewed with an eye towards the possibility of single-chip communication transceivers.

KEYWORDS

resonator, communications, wireless, quality factor, RF MEMS, oscillator, bandpass filter, mixer, transceiver, receiver

1. INTRODUCTION

Due to their need for high frequency selectivity and low noise frequency manipulation, portable wireless communication transceivers continue to rely on off-chip resonator technologies that interface with transistor electronics at the board-level. In particular, highly selective, low loss radio frequency (RF) and intermediate frequency (IF) bandpass filters generally require ceramic, SAW, or quartz acoustic resonator technologies with Q's in excess of 1,000. In addition, LC resonator tanks with Q's greater than 40 are required by voltage-controlled oscillators (VCO's) to achieve sufficiently low phase noise. These off-chip resonator components then contribute to the substantial percentage (often up to 80%) of portable transceiver area taken up by board-level, passive components.

Recent advances in IC-compatible microelectromechanical system (MEMS) technologies that make possible micro-scale, mechanical circuits capable of low-loss filtering, mixing, switching, and frequency generation, now suggest methods for boardless integration of wireless transceiver components. In fact, given the existence already of technologies that merge micromechanics with transistor circuits onto single silicon chips [1]-[8], single-chip transceivers may eventually be possible, perhaps using alternative architectures that maximize
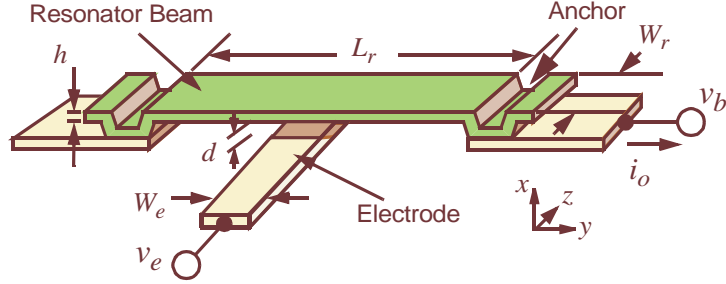
Fig. 1: Perspective-view schematic of a clamped-clamped beam μmechanical resonator in a general bias and excitation configuration.

the use of passive, high-Q, micromechanical circuits to reduce power consumption for portable applications.

This paper presents an overview of the micromechanical circuits and associated technologies expected to play key roles in reducing the size and power consumption of future communication transceivers.

2. MICROMECHANICAL CIRCUITS

Although mechanical circuits, such as quartz crystal resonators and SAW filters, provide essential functions in the majority of transceiver designs, their numbers are generally suppressed due to their large size and finite cost. Unfortunately, when minimizing the use of high-Q components, designers often trade power for selectivity (i.e., Q), and hence, sacrifice transceiver performance.

By shrinking dimensions and introducing batch fabrication techniques, MEMS technology provides a means for relaxing the present constraints on the complexity of mechanical circuits, with implications not unlike those that integrated circuit technology had on transistor circuit complexity [9], [10]. Before exploring the implications, specific μmechanical circuits are first reviewed.

2.1. Micromechanical Beam Element

To date, the majority of μmechanical circuits

most useful for communication functions have been realized using μmechanical flexural-mode beam elements, such as presented in Fig. 1 with clamped-clamped boundary conditions. As shown, this device consists of a beam anchored (i.e., clamped) at both ends, with an electrode underlying its central locations. Both the beam and electrode are constructed of conductive materials, such as doped silicon, or a metal. Although several micromachining technologies are available to realize such an element in a variety of different materials, surface micromachining [11] has so far been the preferred method for μmechanical communication circuits, mainly due to its flexibility in providing a variety of beam end conditions and electrode locations, and its ability to realize very complex geometries with multiple levels of suspension.

As shown in Fig. 1, the μmechanical beam element normally accepts two electrical inputs, v_e and v_b, applied to the electrode and beam, respectively. In this configuration, the difference voltage $(v_e - v_b)$ is effectively applied across the electrode-to-resonator capacitor gap, generating a force between the stationary electrode and movable beam given by

$$F_d = \frac{\partial E}{\partial x} = \frac{1}{2}(v_e - v_b)^2 \frac{\partial C}{\partial x} \qquad (1)$$

where x is displacement (with direction indicated in Fig. 1), and $(\partial C/\partial x)$ is the change in
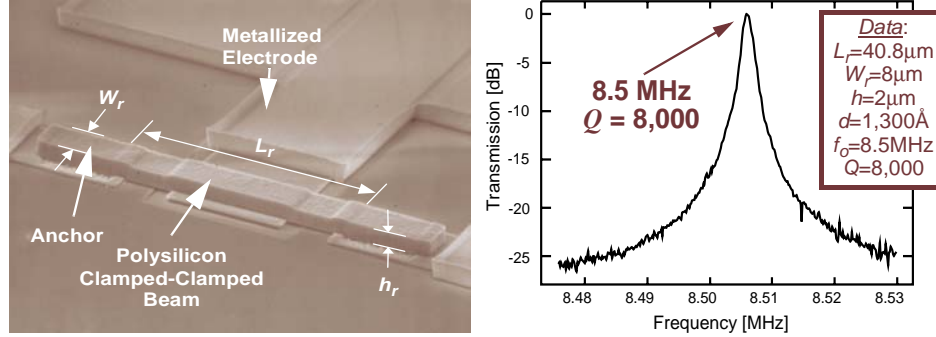
Fig. 2: SEM of an 8.5 MHz clamped-clamped beam μmechanical resonator with a typical measured spectrum [15].

resonator-to-electrode capacitance per unit displacement (and is negative with the directions indicated in Fig. 1). Depending upon the type and frequency of the voltages applied to terminals *e* and *b*, this force can be tailored to specify any one of a variety of signal processing functions available to the beam element. A subset of the most useful of these is now summarized in the following sub-sections.

2.2. Micromechanical Reference Tanks

With Q's in the thousands and ever-improving thermal stabilities, single vibrating μmechanical beam elements are good candidates for use as frequency-setting tanks in reference oscillator applications. When used as a tank or filter circuit (as opposed to a mixer, to be discussed later), a dc-bias voltage $v_b=V_P$ is applied to the conductive beam, while an ac excitation signal $v_e=V_i\cos\omega_i t$ is applied to the underlying electrode. In this configuration, a dominant force component is generated at ω_i, which drives the beam into mechanical resonance when $\omega_i=\omega_o$, creating a dc-biased (via V_P) time-varying capacitance between the electrode and resonator, and sourcing an output current $i_o=V_P(\partial C/\partial x)(\partial x/\partial t)$, as shown in Fig. 1. When plotted versus the frequency of v_i, i_o traces out a bandpass biquad characteristic with a $Q\sim10,000$ in vacuum (c.f., Fig. 2 [15])—very suitable for reference oscillators.

The resonance frequency f_o of a mechanical resonator, such as the clamped-clamped beam of Fig. 1, is governed by both material properties (e.g., Young's modulus, density) and geometry (e.g., length, thickness). For the clamped-clamped beam of Fig. 1, the expression for resonance frequency can be written as (ignoring stress and finite width effects) [15]

$$f_o = \frac{1}{2\pi}\sqrt{\frac{k_r}{m_r}} \cong 1.03\sqrt{\frac{E}{\rho}}\frac{h_{eff}}{L_r^2}(1 - g(V_P))^{1/2} \quad (2)$$

where k_r and m_r are the effective stiffness and mass of the beam at a given location; E and ρ are the Young's modulus and density of the structural material, respectively; L_r is specified in Fig. 1; and h_{eff} is an effective thickness that models the influence of surface topography on the beam in actual implementations, [15], [16]; and the function g models the action of a dc-bias dependent electrical stiffness that adds to mechanical stiffness of the beam, allowing some voltage-control of its frequency. From (2), geometry clearly plays a major role in setting the resonance frequency, and in practice, attaining a specified frequency amounts to CAD layout of the proper dimensions.In general, the resonance frequency of a mechanical resonator increases as its dimensions shrink (e.g., as the length of the beam in Fig. 1 decreases)—thus, the utility of micro- or
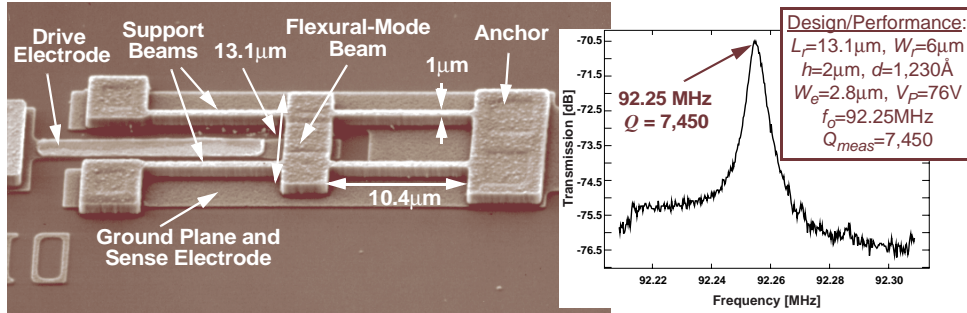
Fig. 3: SEM and measured frequency characteristic for a 92 MHz free-free beam polysilicon μmechanical resonator [23].

nano-scale mechanical resonators for VHF to UHF communication applications.

Although impressive at HF, the clamped-clamped beam device of Fig. 2 begins to lose a substantial fraction of its internal energy to the substrate at frequencies past 30 MHz, and this limits the attainable Q at VHF. One approach to retain high Q as frequencies go beyond 30 MHz is to miniaturize the resonator to the submicron or nano-scale, where its stiffness can be restrained to smaller values so as to reduce energy radiation into the substrate via anchors. Although used successfully to attain mid-VHF frequencies [17], this approach sacrifices the power handling capability (or dynamic range) of the device, possibly rendering it unusable for communications applications where co-site interference is a problem [15], [19], [22]. To retain Q's around 8,000 at VHF while also maintaining a high stiffness for sufficient power handling ability, a beam with free-free ends can be used, such as shown in Fig. 3, in which additional mechanical circuit complexity is added to allow free-free operation, and to reduce anchor losses to the substrate [23]. Via proper support beam design, anchor losses can be greatly attenuated in this structure, and Q's on the order of 8,000 are attained even at 92 MHz. Even higher frequencies should be attainable by either scaling the dimensions of the device in Fig. 3, or by using a higher mode of resonance. Table I presents

Table I: FF-Beam Resonator Freq. Design*

Freq. [MHz]	Material	Mode	h_r [μm]	W_r [μm]	L_r [μm]
70	silicon	1	2	8	14.54
110	silicon	1	2	8	11.26
250	silicon	1	2	4	6.74
870	silicon	2	2	4	4.38
1800	silicon	3	1	4	3.09
1800	diamond	3	1	4	6.16

* Determined for free-free beams using Timoshenko methods that include the effects of finite h and W_r [23].

expected resonance frequencies for various beam dimensions, modes, and structural materials, showing a wide range of attainable frequencies, from VHF to UHF.

Despite evidence in Table I that FF-beams can reach UHF without the need for nano-scale dimensions, there are still lingering concerns associated with scaling these devices, even to the dimensions indicated. In particular, excessive scaling of such devices may increase their susceptibility to "scaling-induced" noise mechanisms, such as contaminant adsorption-desorption noise or thermal fluctuation noise, both of which become increasingly important as dimensions shrink [18]. In addition, excessive scaling can also compromise the power handling capability of these devices [19], making them unsuitable for duplexer or ultra-low phase
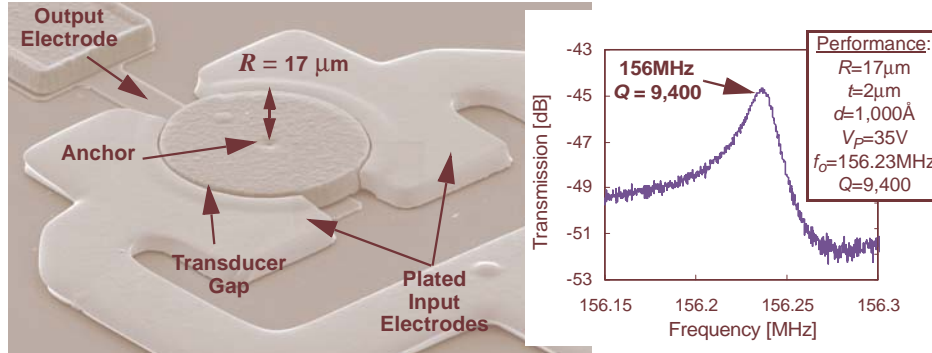
Fig. 4: SEM of a fabricated 156 MHz contour-mode disk μmechanical resonator with a measured frequency characteristic [20].

noise oscillator applications.

With the intent of suppressing the above "scaling-induced" performance limitations, a μmechanical disk resonator, shown in Fig. 4 [20], was recently demonstrated that uses a radial contour (rather than flexural) mode of vibration to attain a mid-VHF frequency of 156 MHz with a Q of 9,400, while still retaining relatively large dimensions. This device consists of a 34μm-diameter, 2μm-thick polysilicon disk suspended by a stem located at its center and enclosed by metal electrodes spaced less than 1,000Å from the disk perimeter. Such tiny lateral electrode-to-resonator gaps were achieved using a recent lateral sub-μm gap process technology that combines surface-micromachining and metal-electroplating technologies with a sacrificial sidewall technique to achieve sub-μm lateral gaps without the need for aggressive lithography or etching [21]. Since the center of the disk corresponds to a node location for the radial contour vibration mode shape, anchor losses through the supporting stem are greatly suppressed, allowing this design to retain a very high Q even at this mid-VHF frequency. With eye on even higher frequencies, Table 2 summarizes needed disk resonator diameters for specific UHF frequencies, showing that UHF is attainable by both polysilicon and polydiamond [13,14] structural materials without the need for sub-μm dimensions.

TABLE 2. μMech. Disk Resonator Design

Freq. [GHz]	Diameter* [μm]	
	polysilicon	polydiamond
0.5	11	20.8
0.8	6.8	13
1	5.4	10.4
2	2.8	5.2

* For the fundamental mode.

2.3. Micromechanical Filters

Among the more useful μmechanical circuits for communications are those implementing low-loss bandpass filters. Figure 5(a) presents the SEM of a two-resonator 68 MHz μmechanical filter, comprised of three mechanical links interconnected in a network designed to yield the bandpass spectrum shown in Fig. 5(b). The design of this filter has been covered extensively in previous literature [15]. For the present purposes, however, the operation of this filter can be deduced from its equivalent circuit, shown in Fig. 5(c). Here, each of the outside links serve as capacitively transduced μmechanical resonators with equivalent circuits based on *LCR* networks. The connecting link actually operates as an acoustic transmission line, and thus, can be modeled by a *T*-network of energy storage elements. When
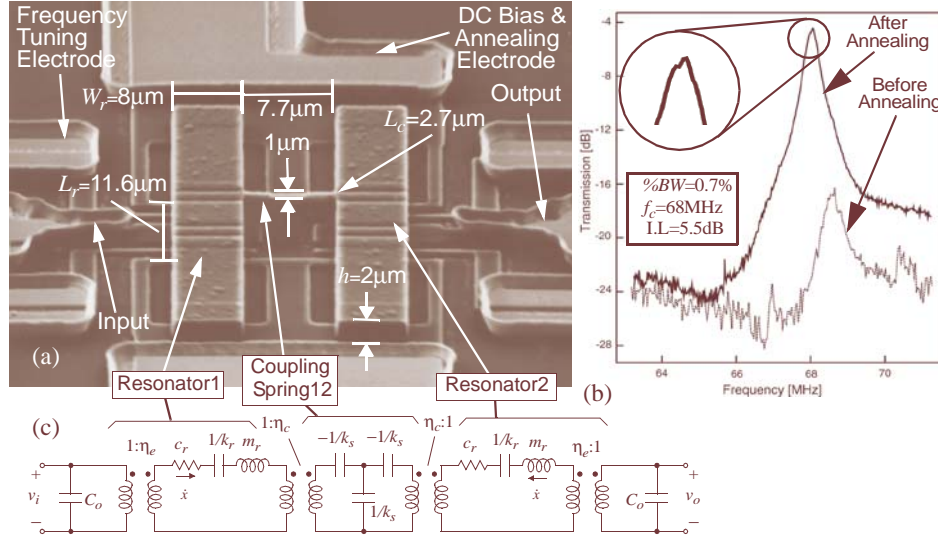
Fig. 5: (a) SEM of a 68 MHz two-resonator μmechanical filter [24]. (b) Measured frequency characteristics. (c) Equivalent circuit [15].

combined together into the circuit of Fig. 5(c), these elements provide a more selective filtering function, with sharper roll-offs and increased stopband rejection over single resonator devices.

Note that Fig. 5 depicts a relatively simple mechanical circuit. Using more complicated interconnections with a larger number of beam elements and I/O ports, a wide variety of signal processing transfer functions can be realized, with even wider application ranges.

2.4. Micromechanical Mixer-Filters

As indicated by (1), the voltage-to-force transducer of Fig. 1 is nonlinear, relating input force F_d to input voltage $(v_e - v_b)$ by a square law. When $v_b = V_P$ (i.e., a dc voltage), this nonlinearity is suppressed, leading to a dominant force that is linear with v_e. If, however, signal inputs are applied to both v_e and v_b, a square law mixer results, that multiplies v_e and v_b, mixing these two input voltages down to a force component at their difference frequency. In particular, if an RF signal v_{RF} at frequency ω_{RF} is

applied to electrode e, and a local oscillator signal v_{LO} at frequency ω_{LO} to electrode b, then these *electrical* signals are mixed down to a *force* signal at frequency $\omega_{IF} = (\omega_{RF} - \omega_{LO})$. If the above transducer is used to couple into a μmechanical filter with a passband centered at ω_{IF} (c.f., Fig. 6), an effective mixer-filter device results that provides both mixing and filtering in one passive, μmechanical device [25]. Since μmechanical circuits exhibit low-loss and consume virtually no dc power, such a device can greatly reduce the power consumption in transceivers, as will soon be seen.

2.5. Micromechanical Switches

The mixer-filter device described above is one example of a μmechanical circuit that harnesses nonlinear device properties to provide a useful function. Another very useful mode of operation that further utilizes the nonlinear nature of the device is the μmechanical switch. Figure 7 presents an operational schematic for a single-pole, single-throw μmechanical switch, seen to have a structure very similar to that of the previous resonator devices: a con-
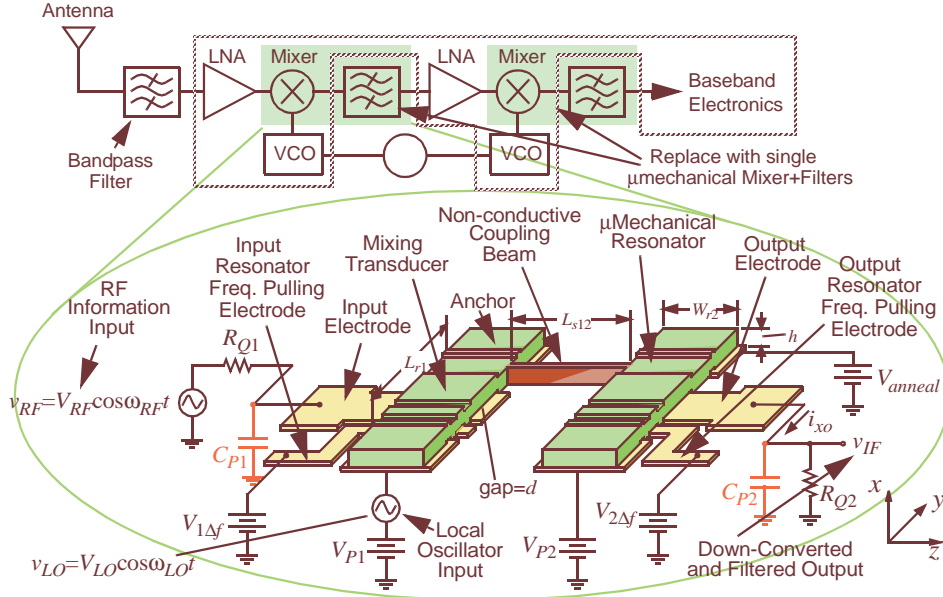
Fig. 6: Schematic diagram of a μmechanical mixer-filter, depicting the bias and excitation scheme needed for down-conversion, and showing its use within a receiver [25].

ductive beam or membrane suspended above an actuating electrode [26]. The operation of the switch of Fig. 7 is fairly simple: To achieve the "on-state", apply a sufficiently large voltage across the beam and electrode to pull the beam down and short it (in either a dc or ac fashion) to the electrode.

In general, to minimize insertion loss, the majority of switches use metals as their structural materials. It is their metal construction that makes μmechanical switches so attractive, allowing them to achieve "on-state" insertion losses down to 0.1 dB—much lower than FET transistor counterparts, which normally exhibit ~2 dB of insertion loss. In addition to exhibiting such low insertion loss, μmechanical switches are extremely linear, with *IIP3*'s greater than 66 dBm [1], and can be designed to consume no dc power (as opposed to FET switches, which sink a finite current when activated).

3. MEMS-BASED TRANSCEIVER ARCHITECTURES

Perhaps the most direct way to harness μmechanical circuits is via direct replacement of the off-chip ceramic, SAW, and crystal resonators used in RF preselect and image reject filters, IF channel-select filters, and crystal oscillator references in conventional super-heterodyne architectures. In addition, μmechanical switches can be used to replace FET T/R switches to greatly reduce wasted power in transmit mode (by as much as 280mW if the desired output power is 500mW). Furthermore, medium-Q micromachined inductors and tunable capacitors [1], [27], [28] can be used in VCO's and matching networks for further miniaturization.

Although beneficial, the performance gains afforded by mere direct replacement by MEMS are quite limited when compared to more aggressive uses of MEMS technology. To fully
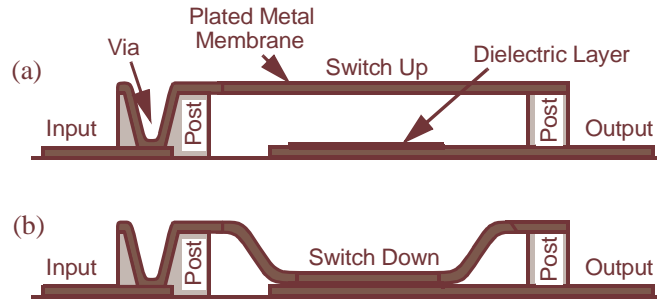
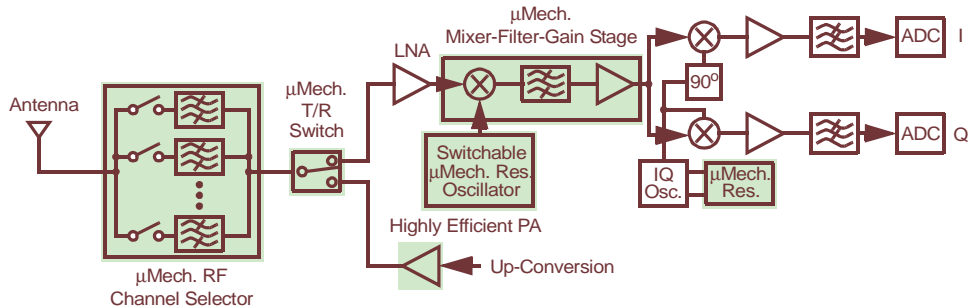Fig. 7: Cross-sectional schematics of a typical μmechanical switch: (a) Switch up. (b) Switch down [26].

Fig. 8: System block diagram for an RF channel-select receiver architecture utilizing large numbers of micromechanical resonators in banks to trade Q for power consumption. (On-chip μmechanics are shaded.)

harness the advantages of μmechanical circuits, one must first recognize that due to their micro-scale size and zero dc power consumption, μmechanical circuits offer the same system complexity advantages over off-chip discrete components that planar IC circuits offer over discrete transistor circuits. Thus, to maximize performance gains, μmechanical circuits should be utilized in large numbers.

Figure 8 presents the system-level block diagram for a possible transceiver front-end architecture that takes full advantage of the complexity achievable via μmechanical circuits [9], [10]. The main driving force behind this architecture is power reduction, attained in several of the blocks by replacing active components by low-loss passive μmechanical ones, and by trading power for high selectivity (i.e.,

high-Q). Among the key performance enhancing features are: (1) an RF channel selector comprised of a bank of switchable μmechanical filters, offering multi-band reconfigurability, receive power savings via relaxed dynamic range requirements [22], and transmit power savings by allowing the use of a more efficient power amplifier; (2) use of a passive μmechanical mixer-filter to replace the active mixer normally used, with obvious power savings; (3) a VCO referenced to a switchable bank of μmechanical resonators, capable of operating without the need for locking to a lower frequency reference, hence, with orders of magnitude lower power consumption than present-day synthesizers; (4) use of a μmechanical T/R switch, with already described power savings in transmit-mode; and (5) use of μmechanical resonator and switch components around the
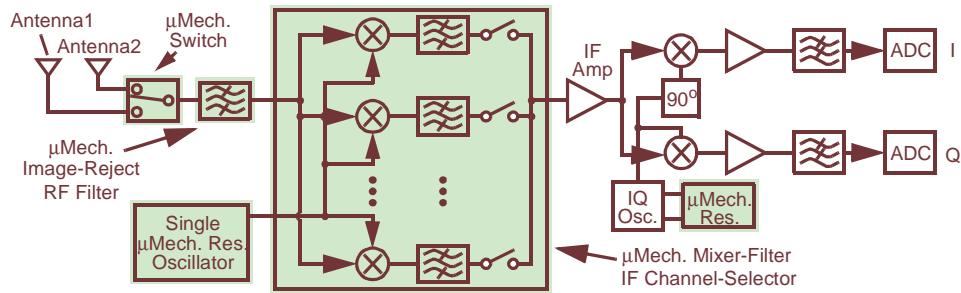
Fig. 9: System block diagram for an all-MEMS receiver front-end, employing an RF image-reject filter, a fixed μmechanical resonator local oscillator, and a switchable array of IF μmechanical mixer-filters.

power amplifier to enhance its efficiency.

Although already quite aggressive, the architecture of Fig. 8 may still not represent the best power savings afforded by MEMS. In fact, even more power savings than in Fig. 8 are possible if the high-Q μmechanical circuits in the signal path can post such low losses that the RF LNA (normally required to boost the received signal against losses and noise from subsequent stages) may in fact no longer be needed. Rather, the RF LNA can be removed, and the needed gain to baseband provided instead by an IF LNA that consumes much less power since it operates at the much lower IF frequency. Without the RF LNA or transistor mixer, the receiver front-end architecture reduces to an all-MEMS topology, such as shown in Fig. 9. Here, since the absence of RF transistor circuits removes dynamic range concerns, the channel-selecting filter bank of Fig. 8 has been converted to a mixer-filter bank and moved down to the IF frequency, where it might be easier to implement, and where it allows the use of a single-frequency RF local oscillator (LO) to down-convert from RF to IF. Since the RF LO is now a single frequency oscillator, power hungry phase-locking and pre-scaling electronics are not needed, allowing similar power advantages as for the VCO in the architecture of Fig. 8. In fact, the architecture of Fig. 9 attains all the power advantages of that of Fig. 8, plus additional power

savings due to the lack of an LNA. It, however, does so at the cost of a slightly higher overall noise figure and decreased robustness against hostile (i.e., jamming) interferers.

4. CIRCUITS/MEMS MERGING TECHNOLOGIES

Although a two-chip solution that combines a MEMS chip with a transistor chip can certainly be used to interface μmechanical circuits with transistor circuits, such an approach becomes less practical as the number of μmechanical components increases. For instance, practical implementations of the switchable filter bank in Fig. 8 require multiplexing support electronics that must interconnect with each μmechanical device. If implemented using a two-chip approach, the number of chip-to-chip bonds required could become quite cumbersome, making a single-chip solution desirable.

In the pursuit of single-chip systems, several technologies that merge micromachining processes with those for integrated circuits have been developed and implemented over the past several years [2]-[8]. Figure 10 presents the cross-section and overhead SEM of one such technology that combined CMOS transistor circuits and polysilicon surface micromachined structures in a fully planar, modular fashion, where transistor and MEMS fabrication steps were separated into modules, and no intermix-
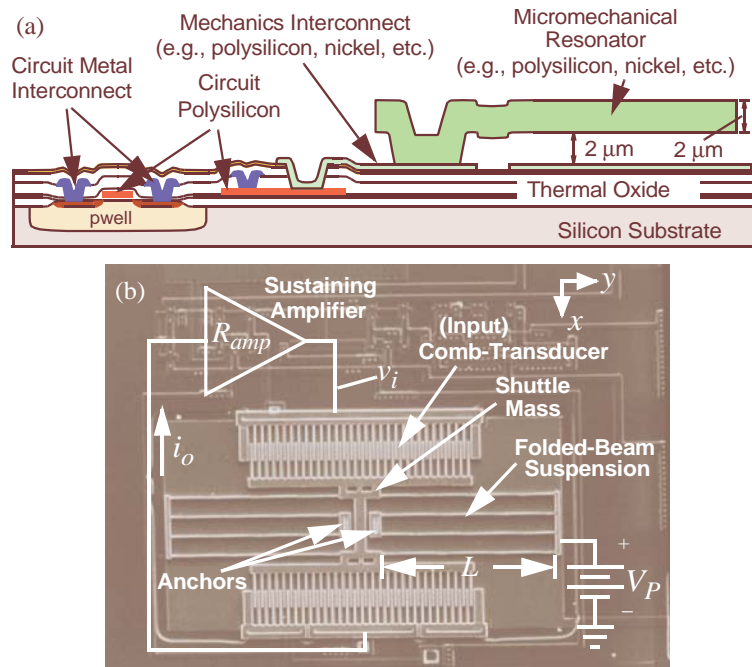
Fig. 10: (a) Cross-section of the MICS process [4]. (b) Overhead-view of a fully integrated micromechanical resonator oscillator fabricated using MICS [12].

ing of process steps from each process was permitted [4], [12]. Such *modular* processes are advantageous, because they allow the greatest flexibility when changes are made to either the transistor or MEMS process steps. (It should be noted that none of the existing fully planar approaches, including the MICS process of Fig. 16, are truly modular, since each requires some degree of sacrifice in either the MEMS or the transistor modules, or both. For example, to circumvent metal-related temperature ceiling limitations when depositing the polysilicon micromechanical material in Fig. 16, the MICS process used tungsten metallization, rather than aluminum. A more modern versions of MICS now allows the use of aluminum metallization, but at the cost of replacing polysilicon with SiGe as the micromechanical material, making high frequency mechanical resonator design more difficult [5].)

In addition to fully planar integration methods, bonding processes, in which circuits and μmechanics are merged by bonding one onto the wafer of the other, are presently undergoing a resurgence [29]. In particular, the advent of more sophisticated aligner-bonder instruments are now making possible much smaller bond pad sizes, which soon may enable wafer-level bonding with bond pad sizes small enough to compete with fully planar processed merging strategies in interface capacitance values. If the bond capacitance can indeed be lowered to this level with acceptable bonding yields, this technology may well be the ultimate in modularity, since it allows the combination of virtually any micromechanical device (e.g., even those made in diamond) with any transistor integrated circuit technology.

Figure 11 presents the cross-section of a recently demonstrated process that combines
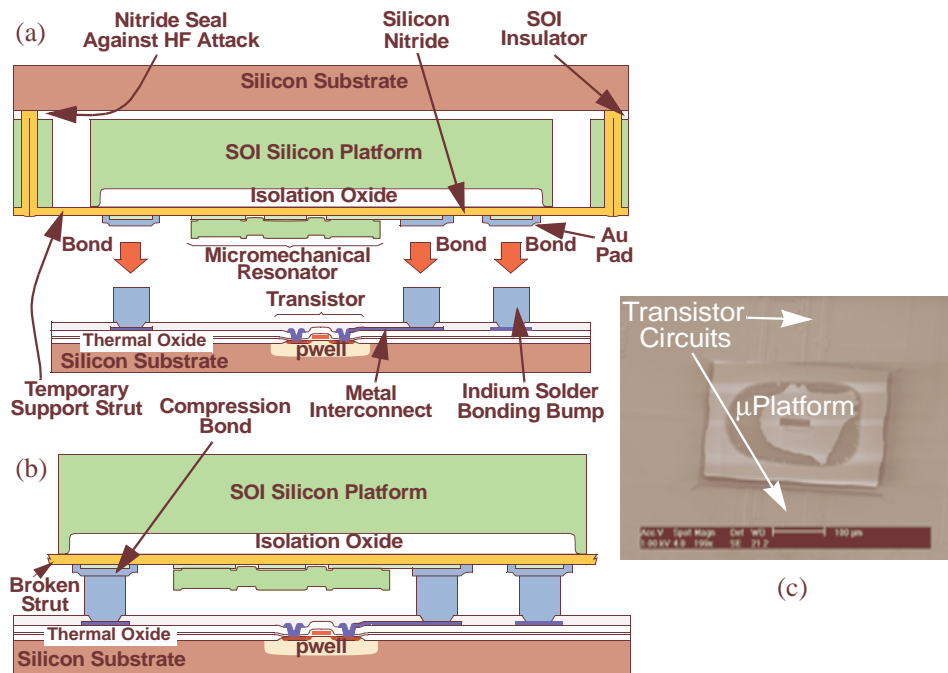
Fig. 11: Illustration of the procedure for achieving a combined MEMS/transsistor chip via the described flip-bond-and-tear process [8]. (a) Bonding. (b) Final cross-section. (c) SEM of a bonded microplatform over CMOS circuits.

micromechanics with transistor circuits using a microplatform bond and transfer approach [8]. In this process, micromechanics are first fabricated onto microplatforms, which are themselves released and suspended over their "MEMS carrier" wafer by temporary tethers. The suspended microplatforms are then flipped and bonded to receiving bond pads on a transistor wafer, then physically torn from the MEMS carrier wafer by breaking the suspending tethers. This bonded platform technology allows low-capacitance, "single-chip", merging of MEMS and transistors with several key advantages: (1) It is truly modular, requiring no compromises in either the MEMS or transistor modules; (2) It attempts to minimize Q-degrading anchor losses experienced by previous bonding-based methods [29] by bonding *platforms* housing resonators, instead of directly

bonding the anchors of resonators; and (3) It constitutes not only a wafer-scale batch approach, but also a repeatable approach, where a step-and-repeat procedure can be used to allow a single MEMS wafer to service several transistor wafers.

From a broader perspective, the integration techniques discussed above are really methods for achieving low capacitance packaging of microelectromechanical systems. As mentioned in Section 2, another level of packaging is required to attain high Q vibrating μmechanical resonators: vacuum encapsulation. Although the requirement for vacuum is unique to vibrating μmechanical resonators, the requirement for encapsulation is nearly universal for all of the μmechanical devices discussed in this paper, and for virtually all micromechanical devices in general. In particu-

lar, some protection from the environment is necessary, even if only to prevent contamination by particles (or even by molecules), or to isolate the device from electric fields or feedthrough currents. Needless to say, wafer-level encapsulation is presently the subject of intense research [30], [31].

5. CONCLUSIONS

Micromechanical circuits attained via MEMS technologies have been described that can potentially play a key role in removing the board-level packaging requirements that currently constrain the size of communication transceivers. In addition, by combining the strengths of integrated μmechanical and transistor circuits, using both in massive quantities, previously unachievable functions become possible that may soon enable alternative transceiver architectures with substantial performance gains, especially from a power perspective. However, before generating too much enthusiasm, it should be understood that RF MEMS technology is still in its infancy, and much research is needed (e.g., on frequency extension, trimming methods, vacuum encapsulation, and much more) before fully-integrated RF MEMS systems can become a reality.

ACKNOWLEDGMENTS

References

[1] C. T.-C. Nguyen, L. P.B. Katehi, and G. M. Rebeiz, "Micromachined devices for wireless communications (invited)," *Proc. IEEE,* vol. 86, no. 8, pp. 1756-1768, Aug. 1998.

[2] T. A. Core, W. K. Tsang, S. J. Sherman, "Fabrication technology for an integrated surface-micromachined sensor," *Solid State Technology*, pp. 39-47, Oct. 1993.

[3] J. H. Smith, S. Montague, J. J. Sniegowski, J. R. Murray, *et al.*, "Embedded micromechanical devices for the monolithic integration of MEMS with CMOS," *Tech. Digest*, IEEE Int. Electron Devices Meeting (IEDM), Washington, D.C., Dec. 10-13, 1995, pp. 609-612.

[4] J. M. Bustillo, G. K. Fedder, C. T.-C. Nguyen, and R. T. Howe, "Process technology for the modular integration of CMOS and polysilicon microstructures," *Microsystem Technologies*, **1** (1994), pp. 30-41.

[5] A. E. Franke, D. Bilic, D. T. Chang, P. T. Jones, T.-J. King, R. T. Howe, and G. C. Johnson, "Post-CMOS integration of germanium microstructures," *Technical Digest*, 12th Int. IEEE MEMS Conf., Orlando, FA, Jan. 17-21, 1999, pp. 630-637.

[6] H. Baltes, O. Paul, and O. Brand, "Micromachined thermally based CMOS microsensors," *Proc. IEEE*, vol. 86, no. 8, pp. 1660-1678, Aug. 1998.

[7] G. K. Fedder, S. Santhanam, M. L. Reed, S. C. Eagle, D. F. Guillou, M. S.-C. Lu, and L. R. Carley, "Laminated high-aspect-ratio microstructures in a conventional CMOS process," *Sensors and Actuators*, vol. A57, no. 2, pp. 103-110, March 1997.

[8] A.-C. Wong, Y. Xie, and C. T.-C. Nguyen, "A bonded-micro-platform technology for modular merging of RF MEMS and transistor circuits," to be published in the *Digest of Technical Papers*, the 11th Int. Conf. on Solid-State Sensors & Actuators (Transducers'01), Munich, Germany, June 10-14, 2001 (4 pages).

[9] C. T.-C. Nguyen, "Micromechanical circuits for communication transceivers (invited)," *Proceedings*, 2000 Bipolar/BiCMOS Circuits and Technology Meeting (BCTM), Minneapolis, Minnesota, September 25-26, 2000, pp. 142-149.

[10] C. T.-C. Nguyen, "Transceiver front-end

architectures using vibrating micromechanical signal processors," to be published in *Low Power Communications Electronics,* edited by G. I. Haddad, T. Itoh, and J. Harvey (35 pages).

[11] J. M. Bustillo, R. T. Howe, and R. S. Muller, "Surface micromachining for microelectromechanical systems (invited)," *Proc. IEEE,* vol. 86, no. 8, pp. 1552-1574, Aug. 1998.

[12] C. T.-C. Nguyen and R. T. Howe, "An integrated CMOS micromechanical resonator high-Q oscillator," *IEEE J. Solid-State Circuits*, vol. 34, no. 4, pp. 440-445, April 1999.

[13] D. Aslam, V. Pappageorgiou, *et al.*, "IC-compatible technology of polydiamond MEMS," *Proceedings*, 6th Annual Symp. on Vehicular Appl. of Displays and Microsensors, Ypsilanti, Michigan, Sept. 22-23, 1999.

[14] M. Aslam and D. Schulz, "Technology of Diamond Microelectromechanical Systems," *Technical Digest*: 8th Int. Conf. Solid-State Sensor & Actuators, Stockholm (Sweden), Vol. 2, 222-224 (1995).

[15] F. D. Bannon III, J. R. Clark, and C. T.-C. Nguyen, "High frequency micromechanical filters," *IEEE J. Solid-State Circuits*, vol. 35, no. 4, pp. 512-526, April 2000.

[16] Q. Meng, M. Mehregany, and R. L. Mullen, "Theoretical modelling of microfabricated beams with elastically restrained supports," *J. Microelectromech. Syst.*, vol. 2, no. 3, pp. 128-137, Sept. 1993.

[17] A. N. Cleland and M. L. Roukes, "Fabrication of high frequency nanometer scale mechanical resonators from bulk Si crystals," *Appl. Phys. Lett.*, **69** (18), pp. 2653-2655, Oct. 28, 1996.

[18] J. R. Vig and Y. Kim, "Noise in microelectromechanical system resonators," *IEEE Trans. Utrason. Ferroelec. Freq. Contr.*, vol. 46, no. 6, pp. 1558-1565, Nov. 1999.

[19] R. Navid, J. R. Clark, M. Demirci, and C. T.-C. Nguyen, "Third-order intermodulation distortion in capacitively-driven CC-beam micromechanical resonators," *Technical Digest*, 14th Int. IEEE Micro Electro Mechanical Systems Conference, Interlaken, Switzerland, Jan. 21-25, 2001, pp. 228-231.

[20] J. R. Clark, W.-T. Hsu, and C. T.-C. Nguyen, "High-Q VHF micromechanical contour-mode disk resonators," *Technical Digest*, IEEE Int. Electron Devices Meeting, San Francisco, California, Dec. 11-13, 2000, pp. 399-402.

[21] W.-T. Hsu, J. R. Clark, and C. T.-C. Nguyen, "A sub-micron capacitive gap process for multiple-metal-electrode lateral micromechanical resonators," *Technical Digest*, 14th Int. IEEE Micro Electro Mechanical Systems Conference, Interlaken, Switzerland, Jan. 21-25, 2001, pp. 349-352.

[22] C. T.-C. Nguyen, "Frequency-selective MEMS for miniaturized low-power communication devices," *IEEE Trans. Microwave Theory Tech.*, vol. 47, no. 8, pp. 1486-1503, Aug. 1999.

[23] K. Wang, A.-C. Wong, and C. T.-C. Nguyen, "VHF free-free beam high-Q micromechanical resonators," *IEEE/ASME J. Microelectromech. Syst.*, vol. 9, no. 3, pp. 347-360, Sept. 2000.

[24] A.-C. Wong, J. R. Clark, and C. T.-C. Nguyen, "Anneal-activated, tunable, 68MHz micromechanical filters" *Digest of Technical Papers*, 10th Int. Conf. on Solid-State Sensors and Actuators, Sendai, Japan, June 7-10, 1999, pp. 1390-1393.

[25] A.-C. Wong, H. Ding, and C. T.-C. Nguyen, "Micromechanical mixer+filters," *Tech. Digest,* IEEE Int. Electron Devices Meeting (IEDM), San Francisco, California, Dec. 6-9, 1998, pp. 471-474.

[26] C. Goldsmith, J. Randall, S. Eshelman, T. H. Lin, D. Denniston, S. Chen and B. Norvell, "Characteristics of micromachined switches at microwave frequencies," IEEE MTT-S Digest, pp. 1141-1144, June, 1996.

[27] D. J. Young and B. E. Boser, "A micromachined variable capacitor for monolithic low-noise VCOs," Technical Digest, 1996 Solid-State Sensor and Actuator Workshop, Hilton Head Island, South Carolina, June 3-6, 1996, pp. 86-89.

[28] J.-B. Yoon, C.-H. Han, E. Yoon, and C.-K. Kim, "Monolithic high-Q overhand inductors fabricated on silicon and glass substrates," *Technical Digest,* IEEE IEDM, Washington, D. C., Dec. 5-8, 1999, pp. 753-756.

[29] A. Singh, D. A. Horsley, M. B. Cohn, A. P. Pisano, and R. T. Howe, "Batch transfer of microstructures using flip-chip solder bonding," *J. Microelectromech. Syst.*, vol. 8, no. 1, pp. 27-33, March 1999.

[30] K. S. Lebouitz, A. Mazaheri, R. T. Howe, and A. P. Pisano, "Vacuum encapsulation of resonant devices using permeable polysilicon," *Technical Digest,* 12th Int. IEEE MEMS Conf., Orlando, Florida, Jan. 17-21, 1999, pp. 470-475.

[31] Y.-T. Cheng, W.-T. Hsu, L. Lin, C. T.-C. Nguyen, and K. Najafi, "Vacuum packaging using localized aluminum/silicon-to-glass bonding," *Technical Digest*, 14th Int. IEEE Micro Electro Mechanical Systems Conference, Interlaken, Switzerland, Jan. 21-25, 2001, pp. 18-21.